Published in final edited form as:
Mol Cancer Ther. 2009 May ; 8(5): 1280–1291. doi:10.1158/1535-7163.MCT-09-0073.

MDA-7/IL-24–induced cell killing in malignant renal carcinoma cells occurs by a ceramide/CD95/PERK–dependent mechanism

Margaret A. Park[1], **Teneille Walker**[1], **Aditi Pandya Martin**[1], **Jeremy Allegood**[1], **Nicollaq Vozhilla**[4], **Luni Emdad**[4], **Devanand Sarkar**[4], **Mohammed Rahmani**[2], **Martin Graf**[3], **Adly Yacoub**[1], **Costas Koumenis**[8], **Sarah Spiegel**[1], **David T. Curiel**[7], **Christina Voelkel-Johnson**[9], **Steven Grant**[1,2,5,6], **Paul B. Fisher**[4,5,6], and **Paul Dent**[1,5,6]

[1] Department of Biochemistry and Molecular Biology, School of Medicine, Virginia Commonwealth University, Richmond, Virginia

[2] Department of Medicine, School of Medicine, Virginia Commonwealth University, Richmond, Virginia

[3] Department of Neurosurgery, School of Medicine, Virginia Commonwealth University, Richmond, Virginia

[4] Department of Human and Molecular Genetics, School of Medicine, Virginia Commonwealth University, Richmond, Virginia

[5] Institute of Molecular Medicine, School of Medicine, Virginia Commonwealth University, Richmond, Virginia

[6] Massey Cancer Center, School of Medicine, Virginia Commonwealth University, Richmond, Virginia

[7] Division of Human Gene Therapy, Departments of Medicine, Pathology and Surgery, and the Gene Therapy Center, University of Alabama at Birmingham, Birmingham, Alabama

[8] Department of Radiation Oncology, University of Pennsylvania School of Medicine, Philadelphia, Pennsylvania

[9] Department of Microbiology and Immunology, Medical University of South Carolina, Charleston, South Carolina

Abstract

Melanoma differentiation associated gene-7/interleukin-24 (*mda-7*/IL-24) is a novel cytokine displaying selective apoptosis-inducing activity in transformed cells without harming normal cells. The present studies focused on clarifying the mechanism(s) by which glutathione *S*-transferase (GST)-MDA-7 altered cell survival of human renal carcinoma cells *in vitro*. GST-MDA-7 caused plasma membrane clustering of CD95 and the association of CD95 with procaspase-8. GST-MDA-7 lethality was suppressed by inhibition of caspase-8 or by overexpression of short-form cellular FLICE inhibitory protein, but only weakly by inhibition of cathepsin proteases. GST-MDA-7–induced CD95 clustering (and apoptosis) was blocked by knockdown of acidic sphingomyelinase or, to a greater extent, ceramide synthase-6 expression. GST-MDA-7 killing was, in parallel, dependent on inactivation of extracellular signal–regulated kinase 1/2 and on

Requests for reprints: Paul Dent, Department of Biochemistry and Molecular Biology, Massey Cancer Center, Virginia Commonwealth University, 401 College Street, Box 980035, Richmond, VA 23298-0035. Phone: 804-628-0861; Fax: 804-827-1309. pdent@vcu.edu.

Disclosure of Potential Conflicts of Interest
No potential conflicts of interest were disclosed.

CD95-induced p38 mitogen-activated protein kinase and c-jun NH_2-terminal kinase-1/2 signaling. Knockdown of CD95 expression abolished GST-MDA-7–induced phosphorylation of protein kinase R–like endoplasmic reticulum kinase. GST-MDA-7 lethality was suppressed by knockout or expression of a dominant negative protein kinase R–like endoplasmic reticulum kinase that correlated with reduced c-jun NH_2-terminal kinase-1/2 and p38 mitogen-activated protein kinase signaling and maintained extracellular signal–regulated kinase-1/2 phosphorylation. GST-MDA-7 caused vacuolization of LC3 through a mechanism that was largely CD95 dependent and whose formation was suppressed by knockdown of ATG5 expression. Knockdown of ATG5 suppressed GST-MDA-7 toxicity. Our data show that in kidney cancer cells GST-MDA-7 induces ceramide-dependent activation of CD95, which is causal in promoting an endoplasmic reticulum stress response that activates multiple proapoptotic pathways to decrease survival.

Introduction

In the United States, renal cell carcinoma (RCC) is diagnosed in ~51,000 patients per annum. If the disease is detected at an early stage, in which a large portion or the entire kidney can be removed with the tumor, a high prolonged level of patient survival is noted (ref. 1 and references therein). However, if the disease has spread to beyond the capsule of the kidney into the adrenal gland or surrounding fascia with nodal involvement, the prognosis is poor with rapid nadir (1). This occurs even under ideal circumstances where the disease is still only locally advanced and essentially all of the tumor can be surgically removed and the patients are maximally treated with radiation and chemotherapy. In part, this is due to the fact that RCC is characterized as frequently being highly refractory to established cytotoxic chemotherapy regimens (1). Collectively, these statistics emphasize the need to develop therapies against this lethal disease that are efficacious and display minimal or optimally no toxicity.

The *mda-7* gene [recently renamed interleukin 24 (IL-24)] was isolated from human melanoma cells induced to terminally differentiate by treatment with fibroblast IFN and mezerein (2). The protein expression of MDA-7/IL-24 is decreased during melanoma progression, with nearly undetectable levels in metastatic disease (2–4). This novel cytokine is classified as a member of the interleukin-10 (IL-10) gene family (5–12). Enforced expression of MDA-7/IL-24, by use of a recombinant adenovirus Ad.*mda-7*, inhibits the growth and kills a broad spectrum of cancer cells, without exerting deleterious effects in normal melanocytes, astrocytes, and human epithelial or fibroblast cells (9–14). Considering its potent cancer-specific apoptosis-inducing ability and tumor growth–suppressing properties in multiple human tumor xenograft animal models, *mda-7*/IL-24 was evaluated in a phase I clinical trial in patients with advanced cancers (10,11,15). This study indicated that Ad. *mda-7* injected intratumorally was safe and with repeated injections instigated significant clinical activity.

The apoptotic pathways by which Ad.*mda-7* causes cell death in tumor cells are not fully understood; however, current evidence suggests an inherent complexity and an involvement of proteins important for the onset of growth inhibition and apoptosis, including BCL-XL, BCL-2, and BAX (9–14). In melanoma cell lines, but not in normal melanocytes, Ad.*mda-7* infection induces a significant decrease in both BCL-2 and BCL-XL levels, with only a modest up-regulation of BAX and BAK expression (16). These data support the hypothesis that Ad.*mda-7* enhances the ratio of proapoptotic to antiapoptotic proteins in cancer cells, thereby facilitating induction of apoptosis (9–14,16). The ability of Ad.*mda-7* to induce apoptosis in DU145 prostate cancer cells, which does not produce BAX, indicates that MDA-7/IL-24 can also mediate apoptosis in tumor cells by a BAX-independent pathway (9–12). In prostate cancer cells, overexpression of either BCL-2 or BCL-XL protects cells from

Ad.*mda-7*–induced toxicity in a cell type–dependent fashion (17). In one ovarian cancer cell line, MDA-7/IL-24 was reported to kill via the extrinsic apoptosis pathway (18). Thus, MDA-7/IL-24 lethality seems to occur by multiple distinct pathways in different cell types, but in all of these studies, cell killing is reflected in a profound induction of mitochondrial dysfunction indicative of intrinsic pathway activation, with relatively modest evidence arguing that MDA-7/IL-24 toxicity can also be linked to the extrinsic pathway of apoptosis signaling.

MDA-7/IL-24 toxicity has been linked to alterations in endoplasmic reticulum stress signaling (19–23). In these studies, MDA-7/IL-24 physically associates with BiP/Grp78 and inactivates the protective actions of this endoplasmic reticulum chaperone protein. In addition to virus-administered *mda-7*/IL-24, delivery of this cytokine as a bacterially expressed glutathione *S*-transferase (GST) fusion protein, GST-MDA-7, retains cancer-specific killing and selective endoplasmic reticulum localization and induces similar signal transduction changes in cancer cells. More recently, we have noted that high concentrations of GST-MDA-7 or infection with Ad.*mda-7* kills primary human glioma cells and does so in a protein kinase R–like endoplasmic reticulum kinase (PERK)–dependent fashion that is dependent on mitochondrial dysfunction but not on activation of the extrinsic pathway (20–23). However, the precise mechanisms by which GST-MDA-7 modulates cell survival in human renal carcinoma cells are presently unknown.

The ability of MDA-7/IL-24 to modulate cell signaling processes in transformed cells has been investigated by several groups (13–28). Our laboratories have shown that Ad. *mda-7* kills melanoma cells, in part, by promoting p38 mitogen-activated protein kinase (MAPK)–dependent activation of the growth arrest and DNA damage inducible genes, including *GADD153*, *GADD45*, and *GADD34* (25). In primary glioblastoma cells, however, we noted that p38 MAPK signaling could also elicit a protective signal (23). Other groups have argued that inhibition of PI3K signaling, but not extra-cellular signal–regulated kinase (ERK)-1/2 signaling, modestly promotes Ad.*mda-7* lethality in breast and lung cancer cells (26,27). Prior work by our groups has shown, using bacterially synthesized GST-MDA-7 protein, that in the 0.25 to 2.0 nmol/L concentration range GST-MDA-7 primarily causes growth arrest with little cell killing, whereas at ~20-fold greater concentrations this cytokine causes profound growth arrest and tumor cell death (22,23,28). Using several established human RCC lines cultured *in vitro*, as well as transformed fibroblasts lacking expression of specific proapoptotic proteins, we currently dissected the effect of GST-MDA-7 on renal cancer cell viability with a focus on elucidating the molecular mechanisms by which GST-MDA-7 enhances cell death.

Materials and Methods

Materials

Transformed PERK$^{-/-}$ cells were a kind gift from Dr. D. Ron (Skirball Institute, NYU School of Medicine, New York, NY). Caspase inhibitors and the cathepsin B inhibitor {[L-3-*trans*-(propylcarbamoyl)oxirane-2-carbonyl]-L-isoleucyl-L-proline methyl ester} were supplied by Calbiochem. Plasmids expressing dominant negative PERK, BiP/Grp78, and LC3-GFP were kindly supplied by Drs. A. Diehl (University of Pennsylvania, Philadelphia, PA), A. Lee (University of California at Los Angeles, Los Angeles, CA), and S. Spiegel (Virginia Commonwealth University, Richmond, VA). Short hairpin RNA constructs targeting *ATG5* (pLVTHM/ATG5) or *Beclin-1* (pSRP-Beclin 1) were generous gifts from Dr. Yousefi (Department of Pharmacology, University of Bern, Bern, Switzerland) and Dr. Yuan (Department of Cell Biology, Harvard Medical School, Boston, MA), respectively. Commercially available validated short hairpin RNA molecules to knock down RNA/protein levels were from Qiagen, as described in refs. 21–23. Antibody reagents,

kinase inhibitors, caspase inhibitors, cell culture reagents, primary human glioblastoma cells, and noncommercial recombinant adenoviruses have been previously described (21–23).

Methods

Synthesis of GST-MDA-7—GST and GST-MDA-7 were generated in bacteria and purified as previously described (28).

Cell Culture and *In vitro* Exposure of Cells to GST-MDA-7 and Drugs—All established RCC lines were cultured at 37°C [5% (v/v) CO_2] *in vitro* using RPMI supplemented with 5% (v/v) FCS and 10% (v/v) nonessential amino acids. The 786-0 lines transfected with empty vector or to express von Hippel Lindau (VHL) were originally generated by Dr. W. Kaelin (Harvard University, Boston, MA). Primary human glioma cells were cultured as described in refs. [22],23. For short-term cell killing assays and immunoblotting, cells were plated at a density of $3 \times 10^3/cm^2$ and, 36 h after plating, were treated with GST-MDA-7 and/or various drugs, as indicated. *In vitro* small-molecule inhibitor treatments were from a 100 mmol/L stock solution of each drug, and the maximal concentration of vehicle (DMSO) in medium was 0.02% (v/v). Cells were not cultured in reduced serum medium during any study (22,23).

Cell Treatments, SDS-PAGE, and Western Blot Analysis—Cells were treated with various GST-MDA-7 concentrations, as indicated in the figure legends. SDS-PAGE and immunoblotting were done as described in refs. [22],[23].

Recombinant Adenoviral Vectors; Infection *In vitro*—We generated and purchased previously noted recombinant adenoviruses as described in refs. [21–23]. Cells were infected with these adenoviruses at an approximate multiplicity of infection as indicated in the figure legend. Cells were incubated for 24 h to ensure adequate expression of transduced gene products before drug exposures.

Detection of Cell Death by Trypan Blue, Hoechst, Terminal Deoxyribonucleotidyl Transferase–Mediated dUTP Nick End Labeling, and Flow Cytometric Assays—Cells were harvested by trypsinization with trypsin/EDTA for ~10 min at 37°C. Cell death assays were done as described in refs. [21–23].

Preparation of S-100 Fractions and Assessment of Cytochrome c Release—Cells were harvested after GST-MDA-7 treatment by centrifugation at 600 rpm for 10 min at 4°C and washed in PBS. Cells (~1×10^6) were lysed by incubation for 3 min in 100 μL of lysis buffer containing digitonin as noted in refs. [21–23]. The lysates were centrifuged at 12,000 rpm for 5 min, and the supernatant was collected and added to an equal volume of 2× Laemmli buffer. The protein samples were quantified and separated by 15% SDS-PAGE.

Plasmid Transfection—Plasmid DNA (0.5 μg/total plasmid transfected) was diluted in 50 μL of RPMI growth medium that lacked supplementation with fetal bovine serum or with penicillin-streptomycin. Lipofectamine 2000 reagent (1 μL; Invitrogen) was diluted into 50 μL growth medium that lacked supplementation with fetal bovine serum or with penicillin-streptomycin. The two solutions were then mixed together and incubated at room temperature for 30 min. The total mix was added to each well (4-well glass slide or 12-well plate) containing 200 μL growth medium that lacked supplementation with fetal bovine serum or with penicillin-streptomycin. The cells were incubated for 4 h at 37°C, after which time the medium was replaced with RPMI growth medium containing 5% (v/v) fetal bovine serum and 1× penicillin-streptomycin.

Microscopy for Acidic Endosomes and LC3-GFP Expression—Where indicated, LC3-GFP–transfected cells, with our without additional siRNA transfection, were pretreated with 3-methyladenine (5 mmol/L; Sigma) 30 min before GST-MDA-7 exposure, then cultured for 12 to 48 h. Cells were then stained with LysoTracker Red dye (Invitrogen) at the indicated time points for 20 min and were visualized immediately after staining on a Zeiss Axiovert 200 microscope using the rhodamine filter. LC3-GFP–transfected cells were visualized at the indicated time points on a Zeiss Axiovert 200 microscope using the FITC filter.

Mass Spectrometric Determination of Ceramide and Dihydroceramide Lipid Levels—UOK121LN cells were treated with 100 nmol/L GST-MDA-7 and were scraped into PBS 6 h after exposure and isolated by centrifugation followed by freezing at −80°C. Lipids were isolated from the cells, and ceramide isoforms analyzed by tandem mass spectrometry (29).

Data Analysis—Comparison of the effects of various treatments was done using one-way ANOVA and two-tailed Student's *t* test. Differences with $P < 0.05$ were considered statistically significant. Experiments shown are the means of multiple individual points from multiple experiments (±SE).

Results

Initial experiments focused on defining the dose-dependent effect of GST-MDA-7 on RCC growth and viability. GST-MDA-7 in a dose-dependent fashion suppressed the proliferation of A498 and UOK121LN cells, but not the proliferation of primary renal epithelial cells (Fig. 1A). These findings correlated with dose-dependent cell killing by GST-MDA-7 in these cells; of note, GST-MDA-7 suppressed tumor cell proliferation without causing a large degree of cell death (Fig. 1B and C; compare Fig. 1A). The majority of RCCs in patients have lost expression of the VHL protein, an E3 ligase, resulting in an increased protein stress load in tumor cells (30). Reexpression of the VHL protein in 786-0 RCCs suppressed the toxicity of GST-MDA-7, which parallels a prior known role of MDA-7/IL-24 in endoplasmic reticulum stress/protein loading signaling (Fig. 1D).

We determined the probable apoptosis mechanism(s) by which GST-MDA-7 promotes cell killing in A498 and UOK121LN cells. Treatment of RCCs with GST-MDA-7 was first noted to induce cell killing ~48 hours after exposure and caused significant cell killing within 72 hours (Fig. 2A). Cell killing was blocked by a pan-caspase inhibitor (zVAD) and an inhibitor of caspase-9 (LEHD) and, in contrast to our prior studies in glioblastoma and prostate cancer cells, also by an inhibitor of caspase-8 (IETD). Similar data were obtained in 786-0 and CAKI cells (data not shown). Cell killing correlated with increased release of cytochrome *c* into the cytosol and with the cleavage of caspase-3 (data not shown). Overexpression of short-form cellular FLICE inhibitory protein (c-FLIP-s) or the viral caspase-8 inhibitor CRM A blocked GST-MDA-7 lethality (Fig. 2B). Knockdown of CD95 or FAS-associated death domain protein (FADD) or caspase-8 or BID expression suppressed GST-MDA-7 lethality (Fig. 2C; data not shown). Treatment of RCCs with GST-MDA-7 promoted a relatively rapid formation of a CD95 death-inducing signaling complex, with a parallel increase in CD95 cell surface localization (Fig. 2D). Treatment of cells with a validated anti–FAS ligand neutralizing antibody (NOK-1) did not alter CD95 activation 6 hours after GST-MDA-7 exposure (data not shown).

Prior studies in glioblastoma cells showed that GST-MDA-7 treatment caused cell killing via a toxic form of autophagy associated with cathepsin B (22,23). In transformed primary mouse fibroblasts, loss of BAX + BAK, BID, or cathepsin B expression significantly

diminished GST-MDA-7 toxicity (Fig. 3A; ref. 31). In contrast to our data in glioblastoma cells, inhibition of cathepsin B very modestly suppressed GST-MDA-7 toxicity in RCCs (Fig. 3B; Supplementary Fig. S1).[10] Similar data were also obtained in 786-0 and CAKI cells (data not shown). Collectively, the data in Figs. 2 and 3 show that GST-MDA-7 activates a CD95-dependent extrinsic pathway to kill RCCs and does not use cathepsin proteases in the killing process.

Recent work from our group noted in glioblastoma cells that GST-MDA-7 caused cell killing by stimulating PERK-dependent toxic autophagy in a CD95-independent fashion. Other findings treating gastrointestinal tumor cell types with the drug combination sorafenib + vorinostat showed that CD95-dependent cell killing was counteracted by CD95-and PERK-dependent protective autophagy (29,32,33). As was observed in glioblastoma cells, GST-MDA-7 caused autophagy and acidic vesicle formation in RCCs as judged by formation of punctate LC3-GFP staining organelles and LysoTracker Red staining, respectively (Fig. 4A). The formation of LC3-GFP vesicles was abolished by the small-molecule inhibitor of autophagy (3-methyladenine), by expression of dominant negative PERK, and by knockdown of either ATG5 or Beclin1 expression, and significantly suppressed by knockdown of CD95 expression (Fig. 4B–D; Supplementary Fig. S2).[10] Similar LC3-GFP vesicularization data to those observed in UOK121LN and A498 cells were also obtained in A498, 786-0, and CAKI cells (data not shown).

Data in Fig. 2C showed that GST-MDA-7 toxicity in RCCs was dependent on CD95, and Fig. 4D showed that GST-MDA-7–induced autophagy was also dependent, in large part, on CD95. These data are consistent with our findings in gastrointestinal tumor cells treated with sorafenib + vorinostat or in primary hepatocytes treated with bile acids (31–33). In Fig. 4C, knockdown of ATG5 abolished GST-MDA-7–induced autophagy, and knockdown of ATG5 reduced GST-MDA-7 lethality by ~60% (Fig. 5A). These findings are also similar to identical studies done in glioblastoma cells where knockdown of either Beclin1 or ATG5 abolished GST-MDA-7–induced autophagy and suppressed cell killing (Supplementary Fig. S3).[10]

In a CD95-dependent fashion, GST-MDA-7 increased PERK and eIF2α phosphorylation and ATG5 expression (Fig. 5B, *top*). GST-MDA-7–induced CD95 death-inducing signaling complex formation was abolished by expression of dominant negative PERK (Fig. 5B, *bottom*). In agreement with data showing that dominant negative PERK blocked death-inducing signaling complex formation, expression of dominant negative PERK abolished GST-MDA-7 toxicity (Fig. 5C). MDA-7 lethality has previously been correlated to the transformation status of cells, with nonestablished primary cells being resistant to the toxic effects of the cytokine (12). GST-MDA-7 lethality in SV40 large T antigen–transformed mouse embryonic fibroblasts, which are not tumorigenic, was enhanced by expression of mutated active K-RAS, which facilitates tumor formation; these toxic effects were reduced in $PERK^{-/-}$ cells (Supplementary Fig. S4).[10]

We have recently reported that drug- or bile acid–induced and ligand-independent CD95 activation is reliant on the actions of both acidic sphingomyelinase (ASMase) and the *de novo* ceramide synthesis pathways (31–33). Knockdown of ASMase or ceramide synthase-6 (LASS6) gene expression in UOK121LN cells prevented CD95 surface localization and cell killing after GST-MDA-7 treatment (Fig. 5D). Similar data were also obtained with myriocin, a small-molecule inhibitor of the *de novo* ceramide synthesis pathway (Fig. 5D; data not shown). GST-MDA-7 treatment in UOK121LN cells significantly ($P < 0.05$) increased C16 ceramide levels 1.23 ± 0.05-fold and increased C16 and C24:1

[10]Supplementary material for this article is available at Molecular Cancer Therapeutics Online (http://mct.aacrjournals.org/).

dihydroceramide levels 1.45 ± 0.05- and 1.33 ± 0.07-fold respectively, within 6 hours of exposure. Collectively, the data in Figs. 4 and 5 show that GST-MDA-7 activates CD95 in a manner that is dependent on the actions of multiple enzymes or pathways that generate ceramide, which promote PERK-dependent cell killing and autophagy.

Finally, we examined the effect of dose-dependent GST-MDA-7 treatment on cell signaling in RCC lines in relation to CD95 and PERK signaling. Low (5 nmol/L) and high (30 nmol/L) doses of GST-MDA-7 initially activate the ERK1/2 pathway; however, high doses of GST-MDA-7 suppressed ERK1/2 activity 48 to 96 hours after treatment (Fig. 6A and B). Low doses, but not high doses, of GST-MDA-7 also activated AKT. Strikingly, high doses of GST-MDA-7, but not low doses of the agent, stimulated activation of the p38α MAPK and c-jun NH_2-terminal kinase (JNK)-1/2 pathways. Based on prior studies that argued either p38α MAPK or JNK1/2 mediated the toxic actions of MDA-7/IL-24 in tumor cells, we made use of small-molecule inhibitors of these enzymes as well as genetic approaches to block signaling. Inhibition of p38α MAPK signaling or JNK1/2 signaling significantly suppressed GST-MDA-7 toxicity (Fig. 6C). Combined inhibition of p38α MAPK and JNK1/2 signaling abolished GST-MDA-7–induced cell death. Knockdown of CD95 or expression of dominant negative PERK significantly suppressed GST-MDA-7–induced activation of JNK1/2 and p38α MAPK and suppressed inactivation of ERK1/2 and the loss of MCL-1 expression (Supplementary Fig. S5).[10]

Overexpression of activated MAPK/ERK kinase 1, to a greater extent than expression of activated AKT, suppressed cell killing by GST-MDA-7 in UOK121LN cells (Fig. 6D). Expression of dominant negative MAPK/ERK kinase 1 or dominant negative AKT enhanced GST-MDA-7 toxicity and interacted in an additive fashion to promote cell death (Supplementary Fig. S6).[10] Thus, GST-MDA-7–induced killing in RCCs was dependent on CD95- and PERK-induced inactivation of ERK1/2 and on CD95- and PERK-induced p38 MAPK and JNK1/2 signaling.

Discussion

Previous studies have shown that GST-MDA-7 reduces proliferation and causes tumor cell–and transformed cell–specific killing and radiosensitization in malignant glioma and prostate cancer cells. However, although JNK signaling plays a key role in radiation-enhanced killing by *mda-7*/IL-24 of tumor cells, the precise signaling pathways provoked by GST-MDA-7 as a single agent and casually related to its cancer-specific cell killing effects in human renal carcinoma cells are still not well understood. The studies in this article were designed to clarify these issues and define how RCCs respond to GST-MDA-7 exposure and how, mechanistically, alterations in multiple signaling pathways affect their cell viability.

A GST-MDA-7 concentration that caused profound toxicity ~72 hours after exposure in RCCs correlated with strong activation of the JNK1/2 and p38 MAPK pathways. This treatment, in parallel, nearly abolished ERK1/2 signaling. Multiple studies using a variety of cytokine and toxic stimuli document that prolonged JNK1/2/3 and/or p38 MAPK activation in a wide variety of cell types can trigger cell death (34,35). The balance between the readouts of ERK1/2 and JNK1/2/3 signaling may also represent a general key homeostatic mechanism that regulates cell survival versus cell death processes (34). Inhibition of either JNK1/2 or p38 MAPK reduced GST-MDA-7 toxicity, and inhibition of both pathways abolished cell killing. Prior work, treating primary hepatocytes with low doses of bile acids, which cause ligand-independent activation of CD95, discovered that JNK1/2 activation was CD95 dependent, and our present studies showed that JNK1/2 and, to a lesser extent, p38 MAPK activation following GST-MDA-7 treatment also required CD95 signaling. CD95 signaling in GST-MDA-7–treated renal carcinoma cells was responsible, in large part, for

PERK activation, and expression of dominant negative PERK blocked MDA-7/IL-24–induced JNK1/2 and p38 MAPK activation as well as the inactivation of ERK1/2. Matsuzawa et al. (36) have previously implicated a tumor necrosis factor receptor–associated factor 2/apoptosis signal–regulating kinase 1/JNK cascade downstream of inositol-requiring enzyme 1 in endoplasmic reticulum stress responses in multiple cell types, and based on our data, PERK-dependent signaling could also feed into this cell survival regulatory process. Collectively, in RCCs MDA-7/IL-24, lethality is reliant on CD95-PERK–dependent JNK1/2 and/or p38 MAPK signaling.

In one ovarian cancer cell line, MDA-7/IL-24, lethality was mediated by CD95-caspase-8 signaling, indicating that the extrinsic pathway to apoptosis could be activated by this cytokine (18). Overexpression of c-FLIP-s or the caspase-8 inhibitory protein CRM A blocked GST-MDA-7 lethality. Knockdown of CD95 or FADD expression similarly reduced GST-MDA-7 toxicity in RCCs. Hence, as was observed in one ovarian line, our findings in RCCs argue that MDA-7/IL-24 toxicity requires death receptor-caspase-8 signaling. However, in all of our prior work with MDA-7/IL-24 in breast, prostate, pancreatic, and brain tumor cells, as well as from the work of others, it was noted that MDA-7/IL-24–induced cell death was mediated by disruption of mitochondrial function with little or no involvement of death receptors or caspase-8 in the killing process. For example, in LNCaP prostate cancer cells, the toxicity of Ad.*mda-7*, either as an individual agent or when combined with a reactive oxygen species–inducing treatment such as ionizing radiation exposure, has been linked to changes in mitochondrial function (17). MDA-7 expression resulted in altered ratios in the expression of proapoptotic BH3 domain–containing proteins, such as BAX, and antiapoptotic proteins, such as BCL-2 and BCL-XL, with the subsequent release of cytochrome *c* into the cytosol followed by activation of caspase-9 and caspase-3 (9–12).

In other cell types that lack expression of BAX, such as DU145, Ad.*mda-7* is an even more potent inducer of tumor cell death than is observed in LNCaP cells. In glioblastoma cells, our data argued that at least five BH3 domain–containing proteins could potentially mediate GST-MDA-7 toxicity downstream of GST-MDA-7–stimulated activation of PERK and JNK1–JNK3 and subsequent reduction in BCL-XL levels (22,23). Our data in RCCs showed that in addition to GST-MDA-7 reducing c-FLIP-s expression, PERK signaling also leads to reduced expression of the short-lived mitochondrial protective protein MCL-1. Collectively, based on these findings, it is tempting to speculate that the reason why multiple transformed cell types exhibit MDA-7/IL-24 toxicity regardless of genetic background is the pleiotropic range of proapoptotic proteins and pathways that can be recruited by this cytokine to initiate mitochondrial cell death processes.

We have recently published several studies arguing that ligand-independent CD95 signaling via PERK promoted both a caspase-8 death signal as well as a counteracting PERK-dependent protective autophagy signal (29,32,33). Others have found that inhibition of caspase-8 can promote a toxic form of autophagy and that the death domain of FADD can promote a toxic form of autophagy when associated with ATG5 in nontransformed cells (37,38). There are three primary unfolded protein response sensors: PERK, activating transcription factor 6, and inositol-requiring enzyme 1. As unfolded proteins accumulate, BiP (Grp78), the heat shock protein-70 endoplasmic reticulum–resident chaperone, dissociates from PERK, activating transcription factor 6, or inositol-requiring enzyme 1. BiP/Grp78 dissociation from PERK allows this protein to dimerize, autophosphorylate, and then phosphorylate eukaryotic translation initiation factor α, the protein required for bringing the initiator methionyl-tRNA to the 40S ribosome (refs. 29,32,33, and references therein). Phosphorylated eIF2α thus leads to repression of global translation, helping to allow cells to recover from the accumulation of unfolded proteins. Reduced translation,

however, can also lower expression of some pro-survival proteins such as MCL-1 and c-FLIP-s, leading to increased cell death (29). In glioma, MDA-7/IL-24 induced PERK-dependent autophagy in a manner not dependent on death receptor or caspase-8 signaling (22,23). GST-MDA-7–induced autophagy in RCCs was significantly, but not fully, suppressed by knockdown of CD95. MDA-7/IL-24 binds to Grp78/BiP, and in glioblastoma cells we initially assumed this binding would play a central role in regulating PERK activity/activation and in causing elevated levels of toxic autophagy, particularly because we subsequently noted that BiP/Grp78 overexpression suppressed MDA-7/IL-24–induced autophagy and cell killing (23). More recently, we also found that overexpression of BiP/Grp78 in RCCs suppressed GST-MDA-7–induced autophagy.[11] Thus, in glioblastoma cells the autophagy being observed after MDA-7/IL-24 treatment is dependent on BiP/Grp78 dysregulation (majority), whereas in RCCs it seems that the autophagy being observed after MDA-7/IL-24 treatment is dependent on both CD95 signaling (majority) and dysregulation of BiP/Grp78 (minority).

In glioblastoma cells, we noted that knockdown of either Beclin1 or ATG5 expression abolished GST-MDA-7–induced autophagy and reduced cell killing. In RCCs, knockdown of either Beclin1 or ATG5 expression also abolished GST-MDA-7–induced autophagy, and knockdown of ATG5 suppressed, but did not abolish, apoptosis. Whether the autophagy induced by GST-MDA-7 through CD95 or through BiP/Grp78 binding represents different survival or toxic signals will need to be defined in a subsequent report. A significant difference between GST-MDA-7–induced cell killing in RCCs and glioblastoma cells was the involvement of cathepsin proteases. In glioblastoma cells, cathepsin proteases were essential for MDA-7/IL-24 lethality, whereas in RCCs, inhibition of cathepsin activity caused only a weak often nonsignificant trend toward lower MDA-7/IL-24 toxicity. It has been shown by many groups that cathepsin proteases play a central role in the biology of glioblastoma, and elevated expression of cathepsin proteases together with reduced expression of cystatins correlates with increased glioblastoma invasiveness and patient morbidity. In contrast, in RCCs expression of cathepsin D has been correlated with an improved long-term patient survival, and cathepsin serum levels do not predict patient disease staging or tumor load (39). These findings again suggest that a reason why MDA-7/IL-24 kills so many transformed cell types, regardless of genetic background, is the diverse range of proapoptotic signals that are recruited by this cytokine to initiate cell death processes.

In our studies, in treating primary hepatocytes with bile acids or RCC/hepatocellular carcinoma/pancreatic tumor cells with the drugs sorafenib and vorinostat, we discovered that ligand-independent activation of CD95 was dependent, in part, on the actions of ASMase and the *de novo* ceramide synthesis pathway (29,32,33). In RCCs, but not glioblastoma cells, GST-MDA-7 caused a ligand-independent activation of CD95 as judged by death-inducing signaling complex formation and CD95 surface localization. In a similar manner to our data with sorafenib and vorinostat in RCCs using siASMase and myriocin, knockdown of ASMase or ceramide synthase-6 expression or treatment with myriocin reduced CD95 activation and reduced cell killing. Recent studies have suggested that the *de novo* and ASMase pathways of ceramide generation can cooperate to regulate lipid raft function (40). Because ceramide synthase 6 and BiP/Grp78 are both endoplasmic reticulum–localized proteins, it is possible that GST-MDA-7, in some manner, by altering endoplasmic reticulum homeostasis, increases ceramide synthase-6 activity, which in RCCs leads to activation of CD95. Understanding how MDA-7/IL-24 regulates ceramide synthase gene function,

[11]Park, Fisher, and Dent, unpublished observations.

ceramide levels, and the roles this lipid may play in the biology of MDA-7/IL-24 will require additional investigations.

At present, MDA-7 is under clinical investigation in phase II trials delivered as a form of gene therapy, Ad.*mda-7* (ING241). In phase I studies in melanoma patients, Ad. *mda-7* generated a significant number of partial and complete responses in patients with metastatic disease, arguing that this cytokine may also promote a vaccination effect in some tumors (12). Because RCC is also known to be responsive to immunomodulatory cytokines, there is a possibility that expression of MDA-7 *in vivo* could promote a vaccination effect in kidney cancer in addition to a tumor-specific cell killing effect. One issue for the use of Ad.*mda-7* (ING241) in renal cancer is that RCCs are largely refractory to infection by type 5 adenovirus, and the development of a tropism-modified adenovirus to express MDA-7 in kidney cancer cells will be required. In conclusion, the present studies offer promise for expanded applications of MDA-7/IL-24 as a generalized and effective therapeutic for RCCs and potentially other cancers. Efforts are being expended to achieve these objectives and also to define clinically useful agents, such as arsenic trioxide or geldanamycins such as 17-*N*-allylamino-17-demethoxygeldanamycin, which, when combined with MDA-7/IL-24, will increase therapeutic benefit for cancer patients.

Supplementary Material

Refer to Web version on PubMed Central for supplementary material.

Acknowledgments

Grant support: USPHS grants P01-CA104177, R01-CA108325, and R01-DK52825, The Jim Valvano “V” Foundation, and Department of Defense Award DAMD17-03-1-0262 (P. Dent); USPHS grants R01-CA63753 and R01-CA77141 and Leukemia Society of America grant 6405-97 (S. Grant); USPHS grants P01-CA104177, R01-CA097318, R01-CA098172, and P01-NS031492, the Samuel Waxman Cancer Research Foundation, and the National Foundation for Cancer Research (P.B. Fisher); and USPHS grant P01-CA104177 (D.T. Curiel). P. Dent is The Universal, Inc. Professor in Signal Transduction Research, and P.B. Fisher is a Samuel Waxman Cancer Research Foundation Investigator.

References

1. Gillett MD, Cheville JC, Karnes RJ, et al. Comparison of presentation and outcome for patients 18 to 40 and 60 to 70 years old with solid renal masses. J Urol 2005;173:1893–6. [PubMed: 15879770]
2. Jiang H, Lin JJ, Su ZZ, Goldstein NI, Fisher PB. Subtraction hybridization identifies a novel melanoma differentiation associated gene, *mda-7*, modulated during human melanoma differentiation, growth and progression. Oncogene 1995;11:2477–86. [PubMed: 8545104]
3. Ekmekcioglu S, Ellerhorst J, Mhashilkar AM, et al. Down-regulated melanoma differentiation associated gene (*mda-7*) expression in human melanomas. Int J Cancer 2001;94:54–59. [PubMed: 11668478]
4. Ellerhorst JA, Prieto VG, Ekmekcioglu S. Loss of MDA-7 expression with progression of melanoma. J Clin Oncol 2002;20:1069–74. [PubMed: 11844832]
5. Huang EY, Madireddi MT, Gopalkrishnan RV, et al. Genomic structure, chromosomal localization and expression profile of a novel melanoma differentiation associated (*mda-7*) gene with cancer specific growth suppressing and apoptosis inducing properties. Oncogene 2001;20:7051–63. [PubMed: 11704829]
6. Parrish-Novak J, Xu W, Brender T, et al. Interleukins 19, 20, and 24 signal through two distinct receptor complexes. Differences in receptor-ligand interactions mediate unique biological functions. J Biol Chem 2002;277:47517–23. [PubMed: 12351624]
7. Caudell EG, Mumm JB, Poindexter N, et al. The protein product of the tumor suppressor gene, melanoma differentiation-associated gene 7, exhibits immunostimulatory activity and is designated IL-24. J Immunol 2002;168:6041–6. [PubMed: 12055212]

8. Pestka S, Krause CD, Sarkar D, Walter MR, Shi Y, Fisher PB. Interleukin-10 and related cytokines and receptors. Annu Rev Immunol 2004;22:929–79. [PubMed: 15032600]
9. Gupta P, Su ZZ, Lebedeva IV, et al. *mda-7*/IL-24: multifunctional cancer-specific apoptosis-inducing cytokine. Pharmacol Ther 2006;111:596–628. [PubMed: 16464504]
10. Lebedeva IV, Sauane M, Gopalkrishnan RV, et al. *mda-7*/IL-24: exploiting cancer's Achilles' heel. Mol Ther 2005;11:4–18. [PubMed: 15585401]
11. Fisher PB, Gopalkrishnan RV, Chada S, et al. *mda-7*/IL-24, a novel cancer selective apoptosis inducing cytokine gene: from the laboratory into the clinic. Cancer Biol Ther 2003;2:S23–37. [PubMed: 14508078]
12. Fisher PB. Is *mda-7*/IL-24 a "magic bullet" for cancer? Cancer Res 2005;65:10128–38. [PubMed: 16287994]
13. Su ZZ, Lebedeva IV, Gopalkrishnan RV, et al. A combinatorial approach for selectively inducing programmed cell death in human pancreatic cancer cells. Proc Natl Acad Sci U S A 2001;98:10332–7. [PubMed: 11526239]
14. Su ZZ, Madireddi MT, Lin JJ, et al. The cancer growth suppressor gene *mda-7* selectively induces apoptosis in human breast cancer cells and inhibits tumor growth in nude mice. Proc Natl Acad Sci U S A 1998;95:14400–5. [PubMed: 9826712]
15. Cunningham CC, Chada S, Merritt JA, et al. Clinical and local biological effects of an intratumoral injection of *mda-7* (IL24; INGN 241) in patients with advanced carcinoma: a phase I study. Mol Ther 2005;11:149–59. [PubMed: 15585416]
16. Lebedeva IV, Su ZZ, Chang Y, Kitada S, Reed JC, Fisher PB. The cancer growth suppressing gene *mda-7* induces apoptosis selectively in human melanoma cells. Oncogene 2002;21:708–18. [PubMed: 11850799]
17. Su ZZ, Lebedeva IV, Sarkar D, et al. Ionizing radiation enhances therapeutic activity of *mda-7*/IL-24: overcoming radiation- and *mda-7*/IL-24-resistance in prostate cancer cells over-expressing the antiapoptotic proteins bcl-x_L or bcl-2. Oncogene 2006;25:2339–48. [PubMed: 16331261]
18. Gopalan B, Litvak A, Sharma S, Mhashilkar AM, Chada S, Ramesh R. Activation of the Fas-FasL signaling pathway by MDA-7/IL-24 kills human ovarian cancer cells. Cancer Res 2005;65:3017–24. [PubMed: 15833826]
19. Gupta P, Walter MR, Su ZZ, et al. BiP/Grp78 Is an intracellular target for MDA-7/IL-24 induction of cancer-specific apoptosis. Cancer Res 2006;66:8182–91. [PubMed: 16912197]
20. Yacoub A, Mitchell C, Hong Y, et al. MDA-7 regulates cell growth and radiosensitivity *in vitro* of primary (non-established) human glioma cells. Cancer Biol Ther 2004;3:739–51. [PubMed: 15197348]
21. Yacoub A, Hamed H, Emdad L, et al. MDA-7/IL-24 plus radiation enhance survival in animals with intracranial primary human GBM tumors. Cancer Biol Ther 2008;7:917–33. [PubMed: 18376144]
22. Yacoub A, Park MA, Gupta P, et al. Caspase-, cathepsin-, and PERK-dependent regulation of MDA-7/IL-24-induced cell killing in primary human glioma cells. Mol Cancer Ther 2008;7:297–313. [PubMed: 18281515]
23. Yacoub A, Gupta P, Park MA, et al. Regulation of GST-MDA-7 toxicity in human glioblastoma cells by ERBB1, ERK1/2, PI3K, and JNK1-3 pathway signaling. Mol Cancer Ther 2008;7:314–29. [PubMed: 18281516]
24. Yacoub A, Mitchell C, Brannon J, et al. MDA-7 (interleukin-24) inhibits the proliferation of renal carcinoma cells and interacts with free radicals to promote cell death and loss of reproductive capacity. Mol Cancer Ther 2003;2:623–32. [PubMed: 12883035]
25. Sarkar D, Su ZZ, Lebedeva IV, et al. *mda-7* (IL-24) Mediates selective apoptosis in human melanoma cells by inducing the coordinated over-expression of the GADD family of genes by means of p38 MAPK. Proc Natl Acad Sci U S A 2002;99:10054–9. [PubMed: 12114539]
26. Mhashilkar AM, Stewart AL, Sieger K, et al. MDA-7 negatively regulates the β-catenin and PI3K signaling pathways in breast and lung tumor cells. Mol Ther 2003;8:207–19. [PubMed: 12907143]
27. Chada S, Bocangel D, Ramesh R, et al. *mda-7*/IL24 kills pancreatic cancer cells by inhibition of the Wnt/PI3K signaling pathways: identification of IL-20 receptor-mediated bystander activity against pancreatic cancer. Mol Ther 2005;11:724–33. [PubMed: 15851011]

28. Sauane M, Gopalkrishnan RV, Choo HT, et al. Mechanistic aspects of *mda-7*/IL-24 cancer cell selectivity analysed via a bacterial fusion protein. Oncogene 2004;23:7679–90. [PubMed: 15334067]
29. Park MA, Zhang G, Martin AP, et al. Vorinostat and sorafenib increase ER stress, autophagy and apoptosis via ceramide-dependent CD95 and PERK activation. Cancer Biol Ther 2008;7:1648–62. [PubMed: 18787411]
30. Turcotte S, Chan DA, Sutphin PD, Hay MP, Denny WA, Giaccia AJ. A molecule targeting VHL-deficient renal cell carcinoma that induces autophagy. Cancer Cell 2008;14:90–102. [PubMed: 18598947]
31. Guicciardi ME, Deussing J, Miyoshi H, et al. Cathepsin B contributes to TNF-α-mediated hepatocyte apoptosis by promoting mitochondrial release of cytochrome *c*. J Clin Invest 2000;106:1127–37. [PubMed: 11067865]
32. Park MA, Zhang G, Norris J, et al. Regulation of autophagy by ceramide-CD95-PERK signaling. Autophagy 2008;4:929–31. [PubMed: 18719356]
33. Zhang G, Park MA, Mitchell C, et al. Multiple cyclin kinase inhibitors promote bile acid-induced apoptosis and autophagy in primary hepatocytes via p53-CD95-dependent signaling. J Biol Chem 2008;283:24343–58. [PubMed: 18614532]
34. Xia Z, Dickens M, Raingeaud J, Davis RJ, Greenberg ME. Opposing effects of ERK and JNK-p38 MAP kinases on apoptosis. Science 1995;270:1326–31. [PubMed: 7481820]
35. Ishizawa J, Yoshida S, Oya M, Mizuno R, Shinojima T, Marumo K, Murai M. Inhibition of the ubiquitin-proteasome pathway activates stress kinases and induces apoptosis in renal cancer cells. Int J Oncol 2004;25:697–702. [PubMed: 15289872]
36. Matsuzawa A, Nishitoh H, Tobiume K, Takeda K, Ichijo H. Physiological roles of ASK1-mediated signal transduction in oxidative stress- and endoplasmic reticulum stress-induced apoptosis: advanced findings from ASK1 knockout mice. Antioxid Redox Signal 2002;4:415–25. [PubMed: 12215209]
37. Yu L, Alva A, Su H, et al. Regulation of an ATG7-beclin 1 program of autophagic cell death by caspase-8. Science 2004;304:1500–2. [PubMed: 15131264]
38. Thorburn J, Moore F, Rao A, et al. Selective inactivation of a Fas-associated death domain protein (FADD)-dependent apoptosis and autophagy pathway in immortal epithelial cells. Mol Biol Cell 2005;16:1189–99. [PubMed: 15635090]
39. Merseburger AS, Hennenlotter J, Simon P, et al. Cathepsin D expression in renal cell cancer—clinical implications. Eur Urol 2005;48:519–26. [PubMed: 16115525]
40. Zhang Y, Li X, Becker KA, Gulbins E. Ceramide-enriched membrane domains—structure and function. Biochim Biophys Acta 2009;1788:178–83. [PubMed: 18786504]

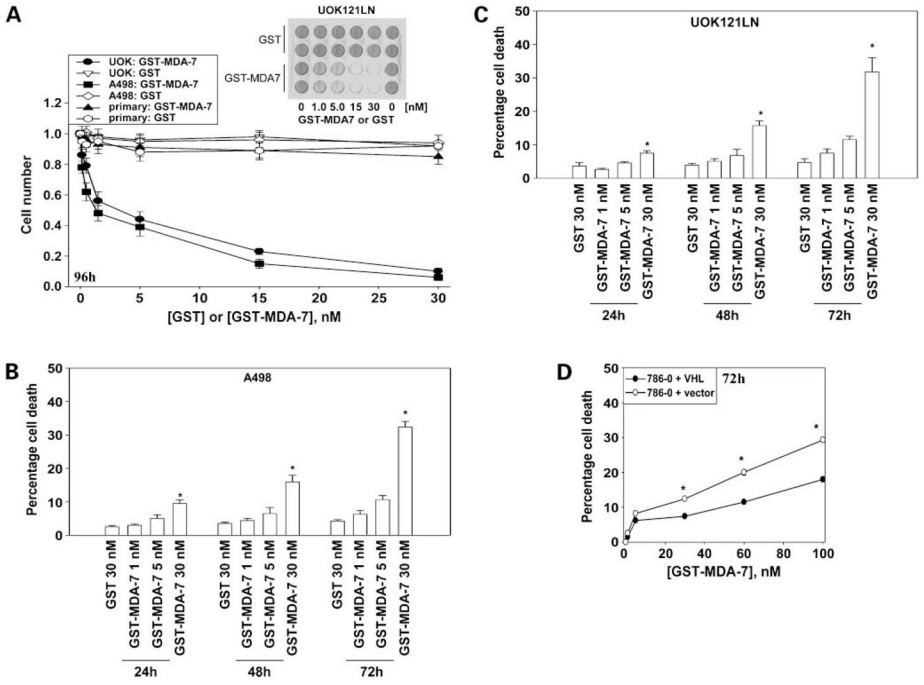

Figure 1.

GST-MDA-7 causes a dose-dependent induction of growth arrest and RCC death. **A,** primary renal epithelial cells, UOK121LN cells, and A498 cells were treated 24 h after plating with GST-MDA-7 (0–30 nmol/L). At the indicated time point after GST-MDA-7 treatment, cell numbers were determined using an 3-(4,5-dimethylthiazol-2-yl)-2,5-diphenyltetrazolium bromide assay ($n = 2$). *Inset*, a scan of a representative plate used in the 3-(4,5-dimethylthiazol-2-yl)-2,5-diphenyltetrazolium bromide assay. **B** and **C,** A498 and UOK121LN cells were treated with 1, 5, or 30 nmol/L of GST-MDA-7/GST 24 h after plating. Cells were isolated 24 to 72 h after exposure and cell viability was determined by Annexin propidium iodide staining assays in triplicate using a flow cytometer (*bars*, SE; $n = 3$). *, $P < 0.05$, greater amount of cell killing than GST-treated cells. **D,** cells (786-0 vector and 786-0 VHL) were cultured for 24 h and then treated with GST-MDA-7 (0–100 nmol/L). Cells were isolated 72 h after GST-MDA-7 treatment and cell viability was determined by trypan blue exclusion assays in triplicate using a hemacytometer (*bars*, SE; $n = 3$). *, $P < 0.05$, greater amount of cell killing in vector control cells.

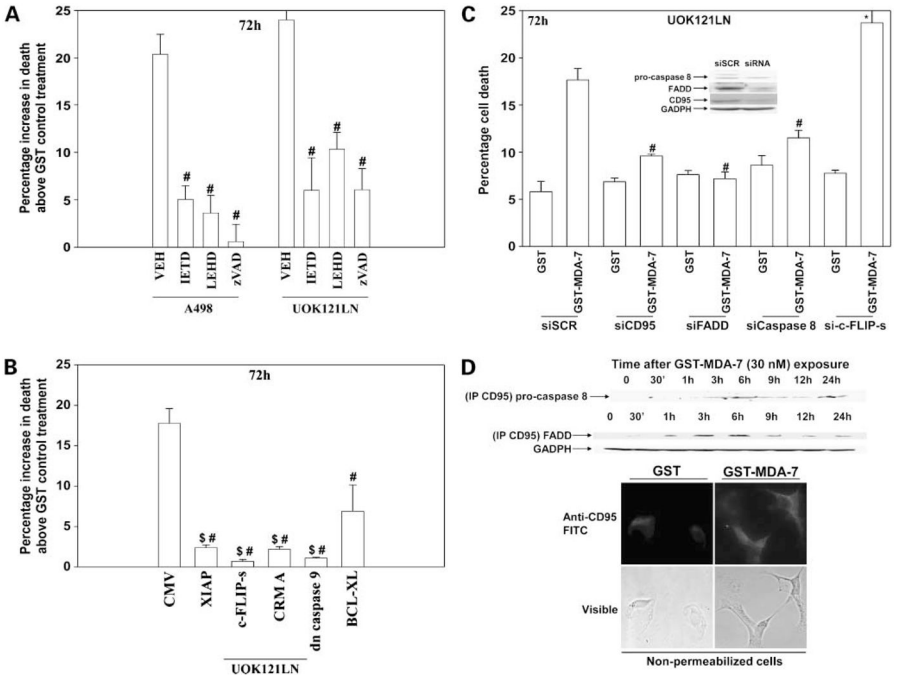

Figure 2.

GST-MDA-7 promotes transformed cell killing through the extrinsic pathway. **A,** A498 or UOK121LN cells were cultured for 24 h and then treated with vehicle (DMSO), the pan-caspase inhibitor zVAD (50 μmol/L), the caspase-9 inhibitor LEHD (50 μmol/L), or the caspase-8 inhibitor IETD (50 μmol/L), followed by treatment with GST or GST-MDA-7 (50 nmol/L). Cells were isolated for viability analyses 72 h after GST-MDA-7 treatment as judged in triplicate by trypan blue dye exclusion assay (*bars*, SE; $n = 3$). #, $P < 0.05$, value less than vehicle-treated cells. **B,** UOK121LN cells were infected (400 multiplicity of infection) with control empty vector virus (CMV) or viruses to express X-linked inhibitor of apoptosis (*XIAP*), c-FLIP-s, CRM A, dominant negative (*dn*) caspase-9, or BCL-XL. Twenty-four hours after infection, cells were treated with GST or GST-MDA-7 (50 nmol/L). Cells were isolated for viability analyses 72 h after GST-MDA-7 treatment as judged in triplicate by trypan blue dye exclusion assay (*bars*, SE; $n = 3$). #, $P < 0.05$, value less than vector-infected cells; $, $P < 0.05$, value less than vector-infected cells. **C,** UOK121LN cells were transfected with siRNA molecules (20 nmol/L) to knock down expression of nothing [siScramble (*siSCR*)], CD95, FADD, caspase-8, or c-FLIP-s. Thirty-six hours after transfection, cells were treated with GST or GST-MDA-7 (50 nmol/L). Cells were isolated for viability analyses 72 h after GST-MDA-7 treatment as judged in triplicate by trypan blue dye exclusion assay (*bars*, SE; $n = 3$). #, $P < 0.05$, value less than siScramble-transfected cells. **D,** *top*, UOK121LN cells were cultured for 24 h and then treated with GST-MDA-7 (50 nmol/L). Cells were isolated 0 to 24 h after treatment and lysed for immunoprecipitation of CD95 followed by assessment of FADD and procaspase-8 levels associated with CD95 using SDS-PAGE. A representative study ($n = 3$) is shown. *Bottom*, UOK121LN cells were plated in four-chambered glass slides and, 24 h after plating, treated with GST or GST-MDA-7 (50 nmol/L). Six hours after treatment, cells were fixed (nonpermeabilized) and immunostained for surface levels of CD95. A representative study ($n = 3$) is shown.

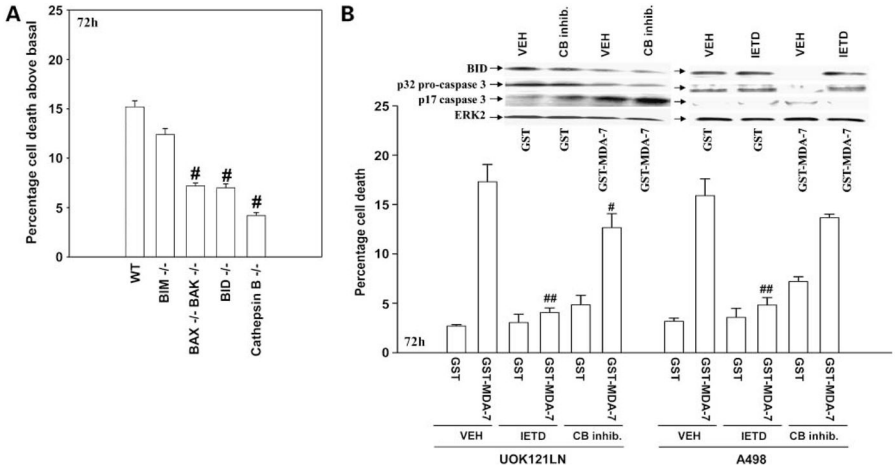

Figure 3.

GST-MDA-7 toxicity in RCCs is dependent on caspase-8 and weakly dependent on cathepsin proteases. **A,** transformed mouse embryonic fibroblasts [wild type (*WT*); deleted for BIM, BID, BAX + BAK, or cathepsin B] were plated and, 24 h later, treated with GST or GST-MDA-7 (100 nmol/L). Cells were isolated for viability analyses 72 h after GST-MDA-7 treatment as judged in triplicate by trypan blue dye exclusion assay (*bars,* SE; $n = 3$). #, $P < 0.05$, value less than vehicle-treated cells. **B,** UOK121LN and A498 cells were treated 24 h after plating with vehicle (DMSO), IETD (50 μmol/L), or cathepsin B inhibitor (*CB inhib.*; 1 μmol/L) followed by treatment with GST or GST-MDA-7 (50 nmol/L). Cells were isolated for viability analyses 72 h after GST-MDA-7 treatment as judged in triplicate by trypan blue dye exclusion assay (*bars,* SE; $n = 3$). #, $P < 0.05$, value less than vehicle-treated cells. *Inset,* immunoblotting of RCCs treated with cathepsin B inhibitor or caspase-8 inhibitor IETD, showing that IETD blocks BID and caspase-3 cleavage in UOK121LN cells ($n = 2$).

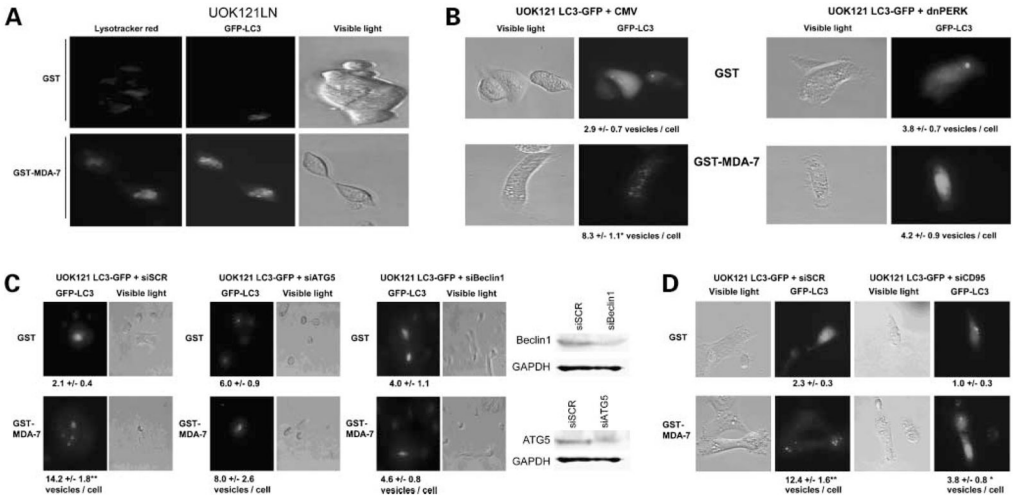

Figure 4.

GST-MDA-7 causes LC3-GFP vacuolization that is blocked by expression of dominant negative PERK or knockdown of CD95, ATG5, or Beclin1. **A,** UOK121LN cells in four-well glass chamber slides in triplicate were transfected with a plasmid to express LC3-GFP and, 24 h after transfection, treated with GSTor GST-MDA-7 (50 nmol/L). Six hours after GST-MDA-7 treatment, LysoTracker Red was added to the culture medium and the cells were examined under visible light or under fluorescent light with appropriate filters (LysoTracker and GFP) at ×40 magnification. The data are representative images from the triplicate plating ($n = 2$). **B,** UOK121LN cells in four-well glass chamber slides in triplicate were transfected with a plasmid to express LC3-GFP in parallel with either a vector control plasmid (CMV) or a plasmid to express dominant negative PERK and, 24 h after transfection, treated with GST or GST-MDA-7 (50 nmol/L). Six hours after GST-MDA-7 treatment, the cells were examined under visible light or under fluorescent light with appropriate filters (LysoTracker and GFP) at ×40 magnification. The data are representative images from the triplicate plating (*bars*, SE; $n = 3$). *, $P < 0.05$, greater than GST control value. **C,** UOK121LN cells in four-well glass chamber slides in triplicate were transfected with a plasmid to express LC3-GFP in parallel with siRNA molecules: an siScramble control, siATG5 to knock down ATG5, or siBeclin1 to knock down Beclin1 expression. Thirty-six hours after transfection, the cells were treated with GSTor GST-MDA-7 (50 nmol/L). Six hours after GST-MDA-7 treatment, the cells were examined under visible light or under fluorescent light with appropriate filters (LysoTracker and GFP) at ×40 magnification. The data are representative images from the triplicate plating (*bars*, SE; $n = 3$). *, $P < 0.05$, greater than GST control value; **, $P < 0.001$, greater than GST control value. **D,** UOK121LN cells in four-well glass chamber slides in triplicate were transfected with a plasmid to express LC3-GFP in parallel with siRNA molecules: an siScramble control and siCD95 to knock down CD95 expression. Thirty-six hours after transfection, the cells were treated with GST or GST-MDA-7 (50 nmol/L). Six hours after GST-MDA-7 treatment, the cells were examined under visible light or under fluorescent light with appropriate filters (LysoTracker and GFP) at ×40 magnification. The data are representative images from the triplicate plating (*bars*, SE; $n = 3$). *, $P < 0.05$, greater than GST control value; **, $P < 0.001$, greater than GST control value.

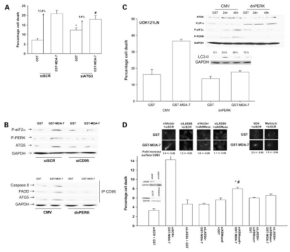

Figure 5.

GST-MDA-7–induced autophagy in RCCs is toxic and is ceramide/CD95/PERK dependent. **A,** UOK121LN cells in triplicate were transfected with siRNA molecules (20 nmol/L): an siScramble control and siATG5 to knock down ATG5 expression. After transfection (36 h), cells were treated with GST or GST-MDA-7 (50 nmol/L). Seventy-two hours after GST-MDA-7 treatment, the cells were isolated for viability analyses as judged in triplicate by trypan blue dye exclusion assay (*bars*, SE; $n = 3$). #, $P < 0.05$, differential value less than vehicle-treated cells. **B,** UOK121LN cells were transfected with either siRNA molecules (20 nmol/L): a siScramble control or siCD95 to knock down CD95 (*top*), or plasmids: an empty vector control plasmid or a plasmid to express dominant negative PERK (*bottom*). Thirty-six hours after transfection, cells were treated with GST or GST-MDA-7 (50 nmol/L). Six hours after GST-MDA-7 treatment, the cells were isolated, and lysates subjected to SDS-PAGE and immunoblotting (*top*) or immunoprecipitation of CD95 followed by SDS-PAGE and immunoblotting ($n = 3$). **C,** UOK121LN cells were transfected with plasmids: an empty vector control plasmid or a plasmid to express dominant negative PERK. Twenty four hours after transfection, cells were treated with GST or GST-MDA-7 (50 nmol/L). Seventy two hours after GST-MDA-7 treatment, the cells were isolated for viability analyses as judged in triplicate by trypan blue dye exclusion assay (*bars*, SE; $n = 3$). *Inset*, transfected cells were isolated 24 to 48 h after GST-MDA-7 treatment and subjected to SDS-PAGE to determine the phosphorylation of PERK/eIF2α and the expression of ATG5, c-FLIP-s, and processed LC3-II ($n = 2$). **D,** UOK121LN cells were transfected with short hairpin siRNA molecules to knock down ASMase expression (20 nmol/L) or a scrambled siRNA or plasmid-expressed siRNA molecules to knock down expression of LASS6 (1 μg). After transfection (36 h), cells were treated with GST or GST-MDA-7 (50 nmol/L). After GST-MDA-7 treatment (72 h), cells were isolated for viability analyses in triplicate by trypan blue (*bars*, SE; $n = 2$). #, $P < 0.05$, less than corresponding value in siScramble cells; *, $P < 0.05$, greater than corresponding value in siLASS6 cells. *Inset*, cells in glass chamber slides were transfected with agents to knock down expression of ASMase and/or LASS6. After transfection (36 h), cells were treated with GST or GST-MDA-7 (50 nmol/L). Six hours after treatment, cells were fixed and surface CD95 levels determined by immunohistochemistry in quadruplicate in unpermeabilized cells using the intensity at 40 separate points per cell (*bars*, SE; $n = 2$).

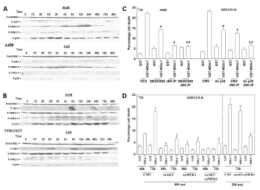

Figure 6.

GST-MDA-7 toxicity in RCCs is mediated by p38 MAPK and JNK1/2 pathway signaling. **A** and **B,** A498 and UOK121LN cells were cultured for 24 h and then treated with GST or GST-MDA-7 (5 or 30 nmol/L, as indicated). Cells were isolated for immunoblotting 0 to 96 h after GST-MDA-7 treatment, and 100 μg of protein at each time point were subjected to SDS-PAGE on 10% gels followed by immunoblotting to determine the total expression of ERK2, P-ERK1/2, P-p38 MAPK, P-JNK1/2, and P-AKT (S473). Representative blots (n = 3). **C,** UOK121LN cells were infected (400 multiplicity of infection) with control empty vector virus (CMV) or a virus to express dominant negative p38α MAPK. Twenty-four hours after infection, cells were treated with vehicle (DMSO) or JNK-IP (10 μmol/L) and then treated with GST or GST-MDA-7 (50 nmol/L). Cells were isolated, and cell viability was determined by trypan blue exclusion assays in triplicate using a hemacytometer. In parallel, A498 cells, 24 h after plating, were treated with vehicle (DMSO), the p38 MAPK inhibitor SB203580 (1 μmol/L), and/or JNK-IP (10 μmol/L) and then treated with GST or GST-MDA-7 (50 nmol/L). Cells were isolated and cell viability was determined by trypan blue exclusion assays in triplicate using a hemacytometer (*bars*, SE; n = 3). #, $P < 0.05$, value less than amount of cell killing in CMV-infected cells; $, $P < 0.05$, value less than amount of cell killing in dominant negative p38 MAPK or JNK-IP treated cells. **D,** UOK121LN cells were infected (400 and 200 multiplicity of infection) with control empty vector virus (CMV), constitutively active (*ca*) AKT, and/or constitutively active MAPK/ERK kinase 1 (*MEK1*). Twenty-four hours after infection, cells were treated with GST or GST-MDA-7 (50 nmol/L). Cells were isolated and cell viability was determined by trypan blue exclusion assays in triplicate using a hemacytometer (*bars*, SE; n = 3). #, $P < 0.05$, value less than amount of cell killing in CMV-infected cells; $, $P < 0.05$, value less than amount of cell killing in constitutively active AKT– and constitutively active MAPK/ERK kinase 1–infected cells.